Curing behavior of epoxy resins with a series of novel curing agents containing 4,4′-biphenyl and varying methylene units

Qing Guo · Yan Huang · Yu-Ying Zhang · Li-Rong Zhu · Bao-Long Zhang

Abstract A new homologous series of curing agents (LCECA*n*) containing 4,4′-biphenyl and *n*-methylene units (*n* = 2, 4, 6) were successfully synthesized. The curing behaviors of a commercial diglycidyl ether of bisphenol-A epoxy (E-51) and 4,4′-bis(2,3-epoxypropoxy)biphenyl (LCE) by using LCECA*n* as the curing agent have been investigated by differential scanning calorimetry (DSC), respectively. The Ozawa equation was applied to the curing kinetics based upon the dynamic DSC data, and the isothermal DSC data were fitted using an autocatalytic curing model. The glass transition temperatures (T_g) of the cured epoxy systems were determined by DSC upon the second heating, and the thermal decomposition temperatures (T_d) were obtained by thermogravimetric (TG) analyses. The results show that the number of methylene units in LCECA*n* has little influence on the curing temperatures of E-51/LCECA*n* and LCE/LCECA*n* systems. In addition, the activation energies obtained by the dynamic method proved to be larger than those by the isothermal method. Furthermore, both the T_g and T_d of the cured E-51/LCECA*n* systems and LCE/LCECA*n* systems decreased with the increase in the number of methylene units in LCECA*n*.

Keywords Curing agent · Curing behavior · Curing kinetics · DSC · TG

Introduction

Epoxy resins are important thermosetting materials and have wide applications in coatings, adhesives, castings, modifiers, and reinforcing materials because of their easy processability and attractive properties such as good strength, good electrical insulation, high adhesion, and good dimensional, thermal, and environmental stabilities. However, their applications are cramped by their brittleness. To solve this problem, intensive investigations with respect to modifications of epoxy resins have been reported by a lot of researchers [1–8]. Additives, fillers, plasticization, toughening, and blending are usually used to modify epoxy resins. Among the various factors affecting the properties of the thermoset resins, the chemical structures of epoxy compounds and curing agents in systems are the most important ones. The influence of the length of aliphatic chains in the curing agents is a point of our interest and has been seldom studied according to our knowledge. Therefore, we designed and synthesized a homologous series of novel curing agents (LCECA*n*) with different number of methylene units (*n* = 2, 4, 6). The curing behaviors of diglycidyl ether of bisphenol-A epoxy (E-51)/ LCECA*n* and 4,4′-bis(2,3-epoxypropoxy)biphenyl (LCE)/ LCECA*n* systems were investigated. In addition, the thermal properties of the cured epoxy/LCECA*n* systems were also discussed.

Another point of our interest is the study of curing kinetics and selection of suitable kinetic model for epoxy/ LCECA*n* curing systems. Information about the kinetics of the curing reaction is useful for the understanding of curing process and the optimization of production [9]. So far, differential scanning calorimetry (DSC) has been widely used for kinetic studies of thermoset curing reactions with a basic assumption that the rate of heat released is

Q. Guo · Y. Huang · Y.-Y. Zhang (✉) · L.-R. Zhu · B.-L. Zhang
Department of Chemistry, Nankai University, Tianjin 300071, China
e-mail: zhangyuying@nankai.edu.cn

proportional to the rate of the curing reaction [10]. A variety of kinetic models or methods have been proposed or employed to investigate kinetic parameters [11–14]. Kissinger proposed an equation for evaluating the kinetic parameters of chemical reaction with differential thermal analysis [15]. Ozawa introduced a method using linear relationship between absolute peak temperature and heating rate without knowing any information about the cure mechanism [16]. Kamal et al. applied a two-parameter autocatalytic model to the cure kinetics of epoxy and unsaturated polyester cure systems [10, 17].

In this article, both the dynamic and isothermal DSC methods were employed. The Ozawa equation was used for the dynamic curing kinetics, and an autocatalytic curing model was chosen for the isothermal DSC data. The kinetic parameters were calculated, and the two methods were compared.

Experimental

Materials

Dimethyl sulfoxide (DMSO) was first stirred with CaH_2 overnight and then distilled under vacuum. Toluene diisocyanate (TDI, 80% 2,4- and 20% 2,6-mixture) was distilled under vacuum before use. 4,4′-dihydroxybiphenyl, 2-bromoethanol, 4-bromo-1-butanol, 6-bromo-1-hexanol, epichlorohydrin, dimethylamine, diglycidyl ether of bisphenol-A epoxy resin (E-51, epoxy equivalent: 196), and all other reagents were obtained commercially and used as received.

Synthesis of 4,4′-bis(2,3-epoxypropoxy)biphenyl (LCE)

The epoxy compound LCE was synthesized according to the reference [18]. Yield: 72%. FT-IR (KBr, cm^{-1}): 2929, 1606, 1501, 1271, 1245, 1036, 911, 816. ^{1}H NMR (CDCl$_3$, ppm): δ7.47 (m, 4H), 6.98 (m, 4H), 4.27 (dd, 2H), 4.00 (dd, 2H), 3.39 (m, 2H), 2.94 (t, 2H), 2.79 (q, 2H). ^{13}C NMR (CDCl$_3$, ppm): δ157.5 (s), 133.9 (s), 127.8 (s), 115.1 (s), 69.5 (s), 51.0 (s), 45.6 (s).

Synthesis of 4,4′-bis(ω-hydroxyalkyloxy)biphenyls (n-BP, n = 2, 4, 6)

As the precursors of the curing agents, n-BP were synthesized from 4,4′-dihydroxybiphenyl, 2-bromoethanol, 4-bromo-1-butanol, and 6-bromo-1-hexanol according to the literature [19]. n = 2: Yield: 75%. FT-IR (KBr, cm^{-1}): 3300, 2934, 2874, 1605, 1500, 1273, 1248, 1092, 1055, 827. ^{1}H NMR (DMSO-d_6, ppm): δ7.53 (d, 4H), 6.99 (d,
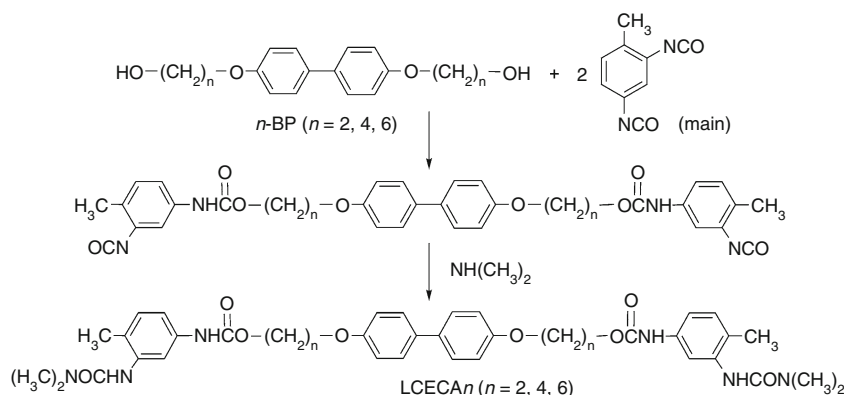
4H), 4.96 (t, 2H), 4.01 (t, 4H), 3.73 (m, 4H). ^{13}C NMR (DMSO-d_6, ppm): δ158.5 (s), 133.0 (s), 127.9 (s), 115.6 (s), 70.3 (s), 60.3 (s). Elem. Anal. Calcd. for $C_{16}H_{18}O_4$: C, 70.06; H, 6.61; Found: C, 69.99; H, 6.58. n = 4: Yield: 70%. FT-IR (KBr, cm^{-1}): 3304, 2945, 2876, 1606, 1500, 1272, 1246, 1076, 1049, 825. ^{1}H NMR (DMSO-d_6, ppm): δ7.51 (d, 4H), 6.97 (d, 4H), 4.46 (t, 2H), 4.00 (t, 4H), 3.46 (m, 4H), 1.75 (m, 4H), 1.57 (m, 4H). ^{13}C NMR (DMSO-d_6, ppm): δ158.5 (s), 133.0 (s), 127.8 (s), 115.5 (s), 68.2 (s), 61.1 (s), 33.2 (s), 29.7 (s), 26.2 (s). Elem. Anal. Calcd. for $C_{20}H_{26}O_4$: C, 72.70; H, 7.93; Found: C, 72.65; H, 7.97. n = 6: Yield: 79%. FT-IR (KBr, cm^{-1}): 3306, 2937, 2866, 1606, 1499, 1272, 1248, 1076, 1042, 825. ^{1}H NMR (DMSO-d_6, ppm): δ7.51 (d, 4H), 6.97 (d, 4H), 4.36 (t, 2H), 3.98 (t, 4H), 3.40 (m, 4H), 1.72 (m, 4H), 1.50–1.30 (m, 12H). ^{13}C NMR (DMSO-d_6, ppm): δ158.5 (s), 133.0 (s), 127.8 (s), 115.5 (s), 68.2 (s), 61.4 (s), 33.2 (s), 29.5 (s), 26.1 (d). Elem. Anal. Calcd. for $C_{24}H_{34}O_4$: C, 74.58; H, 8.87; Found: C, 74.64; H, 8.86.

Synthesis of the curing agents (LCECAn, n = 2, 4, 6) (Scheme 1)

LCECAn were prepared from n-BP, TDI (80/20) and dimethylamine. In a 250-mL, three-necked round-bottom flask equipped with a magnetic stirrer, a mixture of TDI (6 mmol), freshly distilled DMSO (100 mL), and n-BP (2.5 mmol) was stirred for 3 h. A continuous stream of dry nitrogen was bubbled through the mixture all the time. The mixture was heated up slowly to 40 °C and reacted for 3 h. After cooling down to the room temperature, the nitrogen stream was changed to dimethylamine stream and the reaction was maintained for 3 h. The product was then poured into ice water. The obtained precipitate was washed with water, hot isopropanol, and THF, and then dried under vacuum for 48 h to give white powder with a yield of about 70%.

Measurements

IR spectra were recorded on a Bio-Rad FTS-6000 Fourier transform infrared (FT-IR) spectrometer by dispersing the sample in a KBr pellet. ^{1}H NMR spectra were obtained with a Varian UNITY Plus-400 (400 MHz) spectrometer with deuterated chloroform (CDCl$_3$) or dimethyl sulfoxide (DMSO-d_6) as a solvent and tetramethylsilane (TMS) as an internal standard. Liquid-state ^{13}C NMR experiments were carried out on a Varian Mercury Vx300 (75.5 MHz) spectrometer. DSC analyses were performed on a Mettler-Toledo DSC1 in a nitrogen atmosphere at a scanning rate of 10 °C min^{-1}. Thermogravimetric (TG) analyses were carried out on a TG 209 analyzer with a TASC 414/3 controller of Netzsch. The measurements were

Scheme 1 Synthesis of LCECA*n*

performed in a nitrogen atmosphere with a heating rate of 10 °C min^{-1}.

Results and discussion
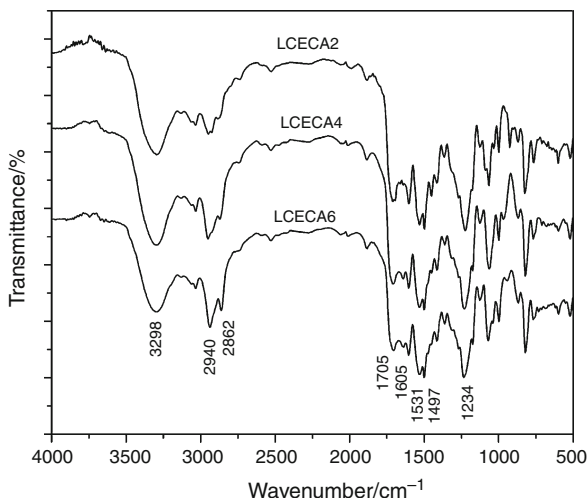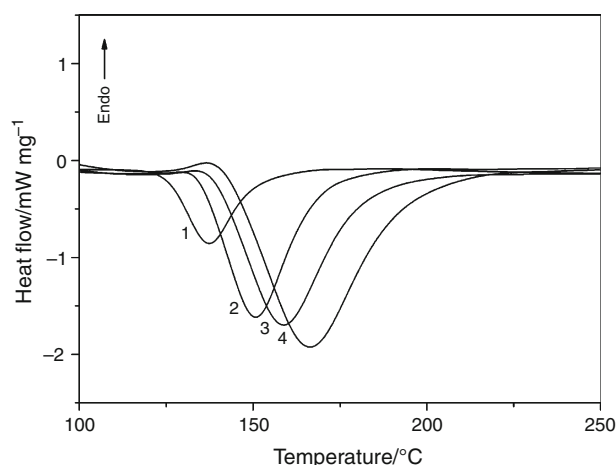
Structural characterization of LCE and LCECA*n*

LCE was structurally characterized by spectroscopic techniques, and its thermal transition was studied by DSC and polarizing microscopy. During the first heating, two endothermic peaks appeared at 135 and 160 °C. On the other hand, only one endothermic peak was found at 159 °C during the second heating, which proved to be the melting point and it agrees with the previous reports [18, 20]. A peak at 911 cm^{-1} was observed in the FT-IR spectrum of LCE, which represents the absorption related to the asymmetric stretch of epoxy ring (Figure not shown).

The FT-IR spectra of LCECA2, LCECA4, and LCECA6 are shown in Fig. 1. For LCECA6, the peaks are assigned as follows: 3298 (N–H), 2940 and 2862 cm^{-1} (–CH$_2$–), 1705 (C=O), 1605 and 1531 (aromatic), 1497 (C–H), 1234

(C–O–C). Both LCECA2 and LCECA4 had spectra quite close to that of LCECA6. As the number of methylene units of LCECA*n* increases, the strength of the peaks at about 2940 and 2862 cm^{-1} increases obviously.

Curing behavior of E-51/LCECA*n*

E-51 and LCECA*n* were mixed well in a 1:1 M ratio, and their curing behaviors were investigated by dynamic and isothermal DSC experiments. Figure 2 shows the dynamic DSC curves of E-51/LCECA2 curing system at a scanning rate of 5, 10, 15, and 20 °C min^{-1}, respectively. All the curves show a single exothermic peak. E-51/LCECA4 and E-51/LCECA6 curing systems proved to show similar dynamic DSC curves. In addition, it is found out that an increase in the number of methylene units in LCECA*n* gives rise to a wider and flatter cure exotherm profile. This behavior suggests that LCECA*n* with longer methylene chain are less reactive. As a result, higher temperature was required for the curing reaction. The curing peak temperatures (T_p) of E-51/LCECA*n* were listed in Table 1, which

Fig. 1 FT-IR spectra of LCECA*n*

Fig. 2 Dynamic DSC curves of E-51/LCECA2 curing system at different heating rates: *1* 5, *2* 10, *3* 15, and *4* 20 °C min^{-1}

Table 1 Dynamic DSC data of E-51/LCECAn and LCE/LCECAn systems

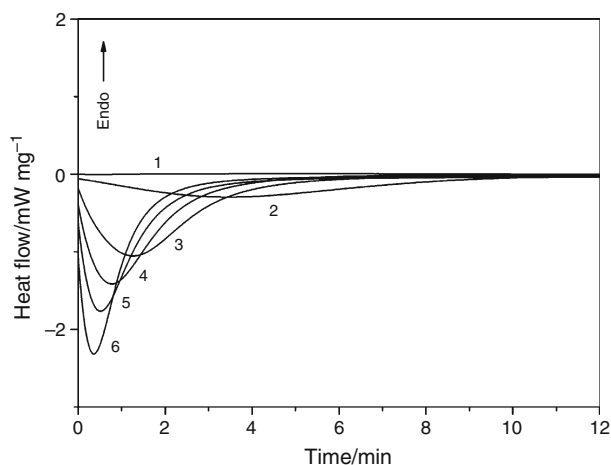| Curing mixture	$T_p/°C$ 5 °C min^{-1}	$T_p/°C$ 10 °C min^{-1}	$T_p/°C$ 15 °C min^{-1}	$T_p/°C$ 20 °C min^{-1}	E_a/kJ mol^{-1}
E-51/LCECA2	137	151	159	167	67
E-51/LCECA4	138	153	164	173	58
E-51/LCECA6	138	152	161	168	66
LCE/LCECA2	145	154	160	165	101
LCE/LCECA4	146	157	166	173	76
LCE/LCECA6	146	156	164	170	85

show that the T_p of E-51/LCECAn systems are rather close at the same heating rate.

According to the Ozawa's study [16], the activation energy can be evaluated from the dynamic DSC data by the following equation:

$$\log \varphi = -0.4567 E_a/RT_p - 2.315 + \log AE_a/R - \log G$$

where φ represents the heating rate/K min^{-1}; T_p represents the peak temperature/K; R is the gas constant. By plotting $\log \varphi$ against $1/T_p$, the E_a values of the E-51/LCECAn systems were then obtained from the slopes and they were listed in Table 1. It can be seen clearly that the E_a values of E-51/LCECAn curing systems are close, and they range from 58 to 67 kJ mol^{-1}.

Figure 3 shows the isothermal DSC curves of E-51/LCECA2 curing system at 100, 120, 140, 150, 160, and 170 °C, respectively. E-51/LCECA4 and E-51/LCECA6 curing systems have similar isothermal DSC curves (Figures not shown). Fractional conversion, α, is defined as $\Delta H_t/\Delta H_o$, where ΔH_t is the area under the plot of dH/dt (i.e., heat flow) against time up to time t, and ΔH_o is the overall heat of reaction determined from dynamic DSC at a constant heating rate [21]. The values of ΔH_o for E-51/LCECA2, E-51/

Fig. 3 Isothermal DSC curves of E-51/LCECA2 curing system at different temperatures: *1* 100, *2* 120, *3* 140, *4* 150, *5* 160, and *6* 170 °C

LCECA4, and E-51/LCECA6 are 173.9, 147.8, and 126.0 J g^{-1}, respectively, measured at the heating rate of 10 °C min^{-1}. Therefore, the diagrams of the reaction rate (i.e., dα/dt) as a function of curing time were then obtained (Figures not shown). All the diagrams show a maximum reaction rate during the curing reaction, except at the start of the reaction, which suggests that an autocatalytic kinetic model is more appropriate for the curing behavior [22]. From these diagrams, the diagrams of fractional conversion α as a function of curing time as well as the diagrams of reaction rate dα/dt as a function of fractional conversion α were then obtained. The autocatalytic kinetic model proposed by Kamal and coworkers [10, 17] is as follows:

$$d\alpha/dt = (k_1 + k_2\alpha^m)(1 - \alpha)^n$$

where k_1 and k_2 are the rate constants with Arrhenius temperature dependency; m and n are the constants independent of temperature. The constant k_1 was obtained from the value of reaction rate at $t = 0$. The kinetic parameters, k_2, m, and n, were obtained with the nonlinear least square method. Based upon the Arrhenius formula, the activation energies, E_{a1} and E_{a2}, were calculated from k_1 and k_2 of different temperatures (140, 150, 160, and 170 °C), respectively, by using the linear regression method. They represent the uncatalyzed and catalyzed curing reaction, respectively [22]. All the kinetic parameters were summarized in Table 2. Obviously, the activation energies for the catalyzed reaction, E_{a2}, are lower in comparison with the E_a calculated by dynamic kinetics. Prime analyzed the DSC methods of the epoxy curing reaction and concluded that the kinetic parameters obtained from dynamic DSC are usually significantly larger than the isothermal [23]. A similar result was reported by Punchaipetch and coworkers [22]. Several authors have investigated the difference between the kinetic parameters obtained from dynamic and isothermal DSC experiments. Riccardi et al. proposed a simple kinetic model for explaining the inconsistencies and reported that the difference was attributed to the curing temperature range difference between isothermal and dynamic methods [24]. Peyser and Bascom pointed out that the initial 10% of the isothermal curing data are not

Table 2 Isothermal kinetic parameters of E-51/LCECAn systems

Curing mixture	k_1/min^{-1}	k_2/min^{-1}	m_{avg}	n_{avg}	E_{a1}/kJ mol^{-1}	E_{a2}/kJ mol^{-1}
E-51/LCECA2	$4.23 \times 10^9 \exp(-10.24/RT)$ $r = 0.9797$	$7.70 \times 10^5 \exp(-5.59/RT)$ $r = 0.9889$	0.68	1.44	85	46
E-51/LCECA4	$4.52 \times 10^{10} \exp(-11.34/RT)$ $r = 0.9549$	$9.68 \times 10^5 \exp(-5.97/RT)$ $r = 0.9913$	0.55	1.10	94	50
E-51/LCECA6	$4.67 \times 10^8 \exp(-9.36/RT)$ $r = 0.8998$	$1.41 \times 10^4 \exp(-4.22/RT)$ $r = 0.9984$	0.50	1.43	78	35
LCE/LCECA2	$1.64 \times 10^{14} \exp(-14.60/RT)$ $r = 0.9042$	$4.22 \times 10^4 \exp(-4.05/RT)$ $r = 0.9736$	0.85	1.65	121	34
LCE/LCECA4	$7.17 \times 10^{11} \exp(-12.49/RT)$ $r = 0.9912$	$2.24 \times 10^4 \exp(-4.15/RT)$ $r = 0.9984$	0.70	1.65	104	34
LCE/LCECA6	$1.22 \times 10^{11} \exp(-11.65/RT)$ $r = 0.9783$	$8.35 \times 10^3 \exp(-3.84/RT)$ $r = 0.9996$	0.58	1.26	97	32

sufficiently accurate because the sample must be heated quickly to the desired temperature [25]. González-Romero and Casillas used DSC data from dynamic and isothermal experiments and a phenomenological model to study the curing kinetics of a thermoset system. It was reported that the differences were attributed to the weakness of the kinetic model rather than the experimental techniques [26].
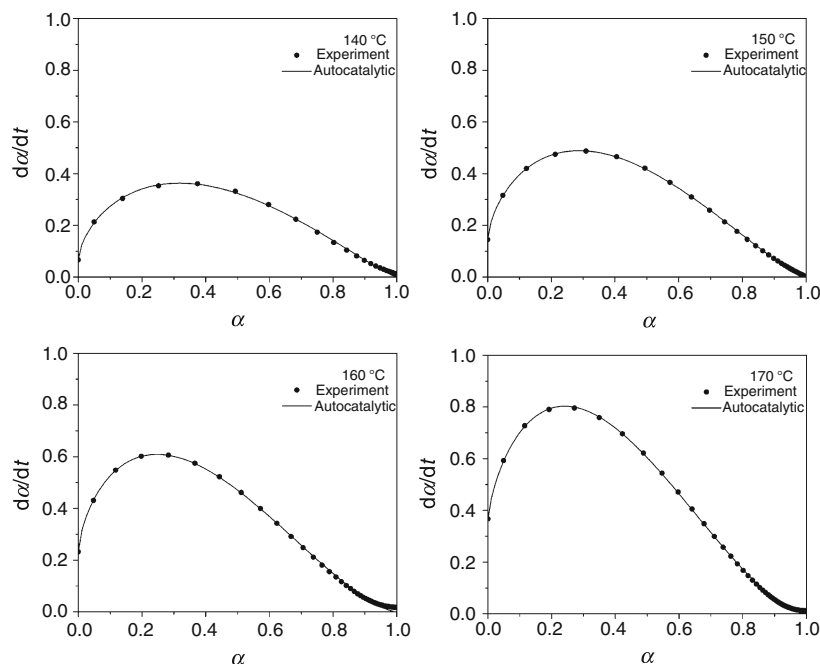
The autocatalytic model investigated here was compared to the experimental data for E-51/LCECAn systems. The comparison for E-51/LCECA2 system was given as a representative case, as shown in Fig. 4. The model fits with the experimental data very well all over the curing reaction at different temperatures. The maximum reaction rate is around 30% conversion. Khanna and Chanda investigated an autocatalytic curing system and found that the
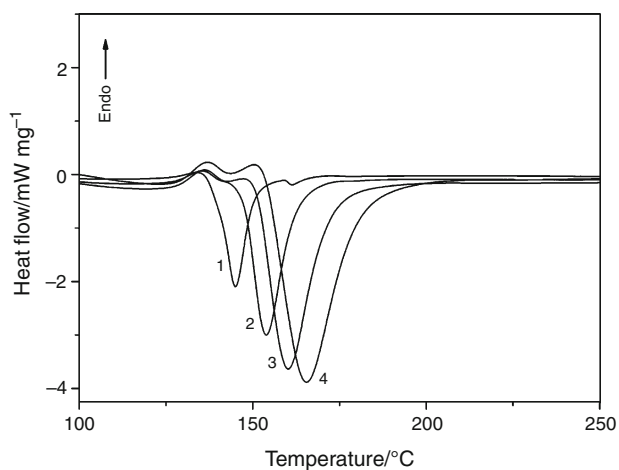
maximum rate of heat evolution generally occurs at 30–40% conversion [27]. Punchaipetch et al. applied the autocatalytic kinetic model proposed by Kamal et al. to their epoxy/anhydride systems, and the maximum reaction rate was found around 20–40% conversion [22].

Curing behavior of LCE/LCECAn

LCE and LCECAn were mixed well in a 1:1 M ratio, and their curing behaviors were investigated by dynamic and isothermal DSC experiments. Figure 5 shows the dynamic DSC curves of LCE/LCECA2 curing system at a scanning rate of 5, 10, 15, and 20 °C min^{-1}, respectively. In addition to the endothermic peaks at about 135 and 150 °C derived from LCE, all the curves show a single exothermic
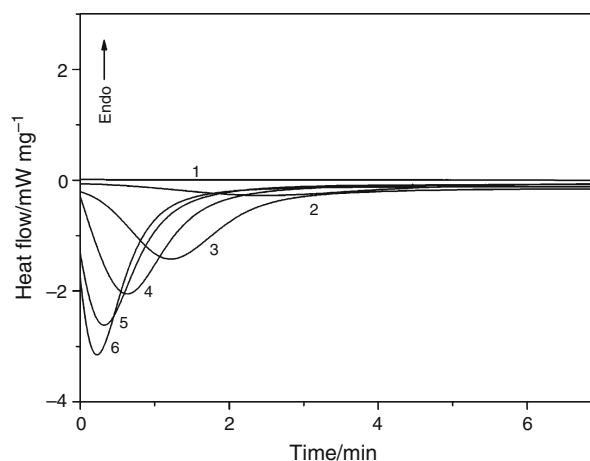

Fig. 4 Comparison of autocatalytic model with experimental data for E-51/LCECA2 system

Fig. 5 Dynamic DSC curves of LCE/LCECA2 curing system at different heating rates: *1* 5, *2* 10, *3* 15, and *4* 20 °C min^{-1}

Fig. 6 Isothermal DSC curves of LCE/LCECA2 curing system at different temperatures: *1* 120, *2* 130, *3* 140, *4* 150, *5* 160, and *6* 170 °C
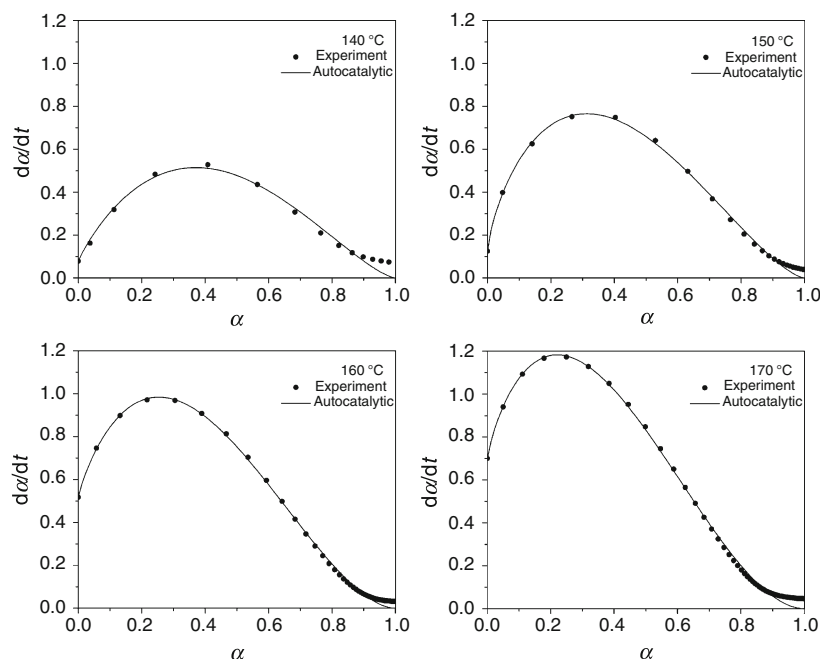
peak. The dynamic DSC curves of LCE/LCECA4 and LCE/LCECA6 curing systems are similar to Fig. 5 (Figures not shown). As the number of methylene units in LCECAn increases, the exothermic peak becomes wider and flatter, indicating a decreasing reactivity of LCECAn. The T_p of LCE/LCECAn were presented in Table 1. It can be seen that LCE/LCECA2, LCE/LCECA4, and LCE/LCECA6 have similar T_p, especially at the low heating rate. According to the Ozawa equation described above, the E_a of LCE/LCECAn systems were obtained and also presented in Table 1. The E_a of LCE/LCECA4 and LCE/LCECA6 are 76 and 85 kJ mol^{-1}, respectively, while the value for LCE/LCECA2 is higher.

LCE/LCECAn curing systems have similar isothermal DSC curves at the same temperature. Figure 6 shows the isothermal DSC curves of LCE/LCECA2 at 120, 130, 140, 150, 160, and 170 °C, respectively. The values of ΔH_o for LCE/LCECA2, LCE/LCECA4, and LCE/LCECA6 are 160.5, 146.3, and 141.4 J g^{-1}, respectively, measured by dynamic DSC at the heating rate of 10 °C min^{-1}. The diagrams of reaction rate dα/dt as a function of fractional conversion α were obtained and then fitted as mentioned above for E-51/LCECAn systems. The resulting kinetic parameters were listed in Table 2. The activation energies for the catalyzed reaction, E_{a2}, are very close and much lower than the E_a calculated by dynamic kinetics.

Fig. 7 Comparison of autocatalytic model with experimental data for LCE/LCECA2 system

Table 3 Thermal properties of the cured epoxy resins

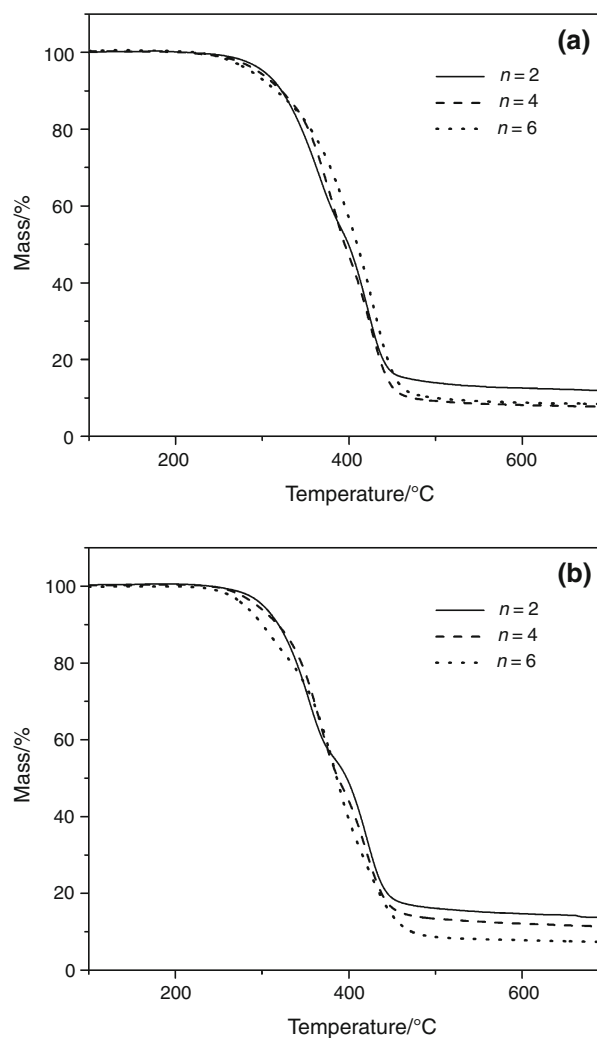| Sample[a]	T_g/°C	T_d/°C	Sample[a]	T_g/°C	T_d/°C
E-51/LCECA2	124	302	LCE/LCECA2	136	301
E-51/LCECA4	100	296	LCE/LCECA4	117	294
E-51/LCECA6	94	287	LCE/LCECA6	97	280

[a] Pre-cured at 140 °C for 2 h and post-cured at 160 °C for 2 h

The fitting curves of the autocatalytic model were compared to the experimental data for LCE/LCECA*n* systems. The comparison for LCE/LCECA2 system was given as a representative case, as shown in Fig. 7. The model fits with the experimental data well from the beginning of the curing reaction to about 90% conversion. The maximum reaction rate is around 30% conversion.

Thermal properties of the cured epoxy resin*s*

The glass transition temperatures (T_g) of the cured epoxy resins were determined by DSC upon the second heating with a rate of 10 °C min^{-1}. The data are recorded in Table 3. The T_g of the cured E-51/LCECA2 and LCE/LCECA2 is 124 and 136 °C, respectively, and this value drops to 94 and 97 °C as the number of the methylene units (*n*) rises to 6. Many literatures have reported the effect of crosslinking on T_g. It was proved by Hale et al. that the T_g of thermosetting polymers rose with the increase in crosslink density [28]. In this study, an increase in the number of the methylene units lengthened the segment between crosslink junctions, which led to the decrease in the crosslink density of the resulting epoxy thermosets.

The thermal stabilities of the cured epoxy resins were determined in nitrogen by TG at a heating rate of 10 °C min^{-1}. Figure 8 shows the decomposition curves of the cured E-51/LCECA*n* and LCE/LCECA*n*. All the temperatures of 5% mass loss (T_d) were listed in Table 3. LCECA*n* containing longer methylene chains endows the E-51/LCECA*n* sample with a lower T_d. The T_d of the cured LCE/LCECA*n* has the same tendency. They decrease from 301 to 280 °C with increasing the number of the methylene units in LCECA*n*. This result is probably because of the decrease in the crosslink density. The correlation of thermal stability with crosslink density of polymer networks has been investigated by some researchers. The effect of crosslink density on thermal stability of the NR/PS interpenetrating polymer networks was studied by Mathew and coworkers. They found out that the thermal stability was enhanced on increasing the crosslink density, because the energy required for bond scission and volatilization of products is higher at high crosslink density [29]. Gupta et al. reported that an increase in crosslink density causes

Fig. 8 TG curves of the cured E-51/LCECA*n* and LCE/LCECA*n* in nitrogen with a heating rate of 10 °C/min: **a** E-51/LCECA*n* and **b** LCE/LCECA*n*

chain stiffen and results in increased thermal stability of the DGEBA/polycaprolactam system [30].

Conclusions

E-51/LCECA*n* (*n* = 2, 4, 6) systems had similar curing temperatures. The activation energies obtained from dynamic DSC data ranged from 58 to 67 kJ mol^{-1}, and the catalyzed values from isothermal kinetics E_{a2} were between 35 and 50 kJ mol^{-1}. The autocatalytic model fitted well with the isothermal experimental data over the curing reaction at different test temperatures.

LCE/LCECA*n* (*n* = 2, 4, 6) systems also had similar curing temperatures. The activation energies estimated by dynamic kinetics ranged from 76 to 101 kJ mol^{-1}, and the activation energies for the catalyzed reaction E_{a2} ranged from 32 to 34 kJ mol^{-1}. The autocatalytic model fitted

well with the experimental data from the beginning of the curing reaction to about 90% conversion.

For both E-51/LCECAn and LCE/LCECAn systems, LCECAn with longer methylene chain were less reactive. The values of activation energies obtained by dynamic method were larger than those by isothermal method. Moreover, the T_g and thermal stabilities of the cured E-51/LCECAn and LCE/LCECAn decreased with increasing the number of the methylene units in the curing agents.

References

1. Zhang B-L, Tang G-L, Shi K-Y, You Y-C, Du Z-J, Yang J-F, et al. A study on properties of epoxy resin toughened by functionalized polymer containing rigid, rod-like moiety. Eur Polym J. 2000;36:205–13.
2. He S, Shi K, Bai J, Zhang Z, Li L, Du Z, et al. Studies on the properties of epoxy resins modified with chain-extended ureas. Polymer. 2001;42:9641–7.
3. He SJ, Shi KY, Guo XZ, Du ZJ, Zhang BL. Properties of methyltetrahydrophthalic anhydride-cured epoxy resin modified with MITU. Polym Adv Technol. 2009;20:130–4.
4. Zhang B-L, Tang G-L, Shi K-Y, You Y-C, Du Z-J, Huang J-F. A study on the properties of epoxy resin toughened by a liquid crystal-type oligomer. J Appl Polym Sci. 1999;71:177–84.
5. Ma S, Liu W, Su Q, Liu Y. Studies on the thermal properties of epoxy resins modified with two kinds of silanes. J Macromol Sci: Phys. 2010;49:43–56.
6. Villanueva M, Fraga I, Rodríguez-Añón J, Proupín-Castiñeiras J. Study of the influence of a reactive diluent on the rheological properties of an epoxy-diamine system. J Therm Anal Calorim. 2009;98:521–5.
7. Villanueva M, Martín-Iglesias J, Rodríguez-Añón J, Proupín-Castiñeiras J. Thermal study of an epoxy system DGEBA (n = 0)/mXDA modified with POSS. J Therm Anal Calorim. 2009;96:575–82.
8. López J, Rico M, Montero B, Díez J, Ramírez C. Polymer blends based on an epoxy-amine thermoset and a thermoplastic. J Therm Anal Calorim. 2009;95:369–76.
9. Yousefi A, Lafleur PG, Gauvin R. Kinetic studies of thermoset cure reactions: a review. Polym Compos. 1997;18:157–68.
10. Kamal MR. Thermoset characterization for moldability analysis. Polym Eng Sci. 1974;14:231–9.
11. Batch GL, Macosko CW. Kinetic model for crosslinking free radical polymerization including diffusion limitations. J Appl Polym Sci. 1992;44:1711–29.
12. Patel PS, Shah PP, Patel SR. Differential scanning calorimetry investigation of curing of bisphenolfurfural resins. Polym Eng Sci. 1986;26:1186–90.
13. Vinnik R, Roznyatovsky V. Kinetic method by using calorimetry to mechanism of epoxy-amine cure reaction. J Therm Anal Calorim. 2003;73:807–17.
14. Liu X, Sheng X, Lee J, Kessler M. Isothermal cure characterization of dicyclopentadiene. J Therm Anal Calorim. 2007;89:453–7.
15. Kissinger HE. Reaction kinetics in differential thermal analysis. Anal Chem. 1957;29:1702–6.
16. Ozawa T. Kinetic analysis of derivative curves in thermal analysis. J Therm Anal Calorim. 1970;2:301–24.
17. Kamal MR, Sourour S. Kinetics and thermal characterization of thermoset cure. Polym Eng Sci. 1973;13:59–64.
18. Mormann W, Bröcher M. "Liquid crystalline" thermosets from 4,4′-bis(2, 3-epoxypropoxy)biphenyl and aromatic diamines. Macromol Chem Phys. 1996;197:1841–51.
19. Ando M, Uryu T. Synthesis of polymer materials by low energy electron beam. XIII. Structure and properties of EB-cured polymers of bifunctional monomer with biphenyl moiety as mesogenic group. J Polym Sci A: Polym Chem. 1990;28:2575–84.
20. Giamberjni M, Amendola E, Carfagna C. Liquid crystalline epoxy thermosets. Mol Cryst Liq Cryst. 1995;266:9–22.
21. Barton JM. Monitoring the curing reaction of an aromatic amine/epoxide resin system by differential scanning calorimetry (DSC): determination and significance of the activation energy. Makromol Chem. 1973;171:247–51.
22. Punchaipetch P, Ambrogi V, Giamberini M, Brostow W, Carfagna C, D'Souza NA. Epoxy + liquid crystalline epoxy coreacted networks: I. Synthesis and curing kinetics. Polymer. 2001;42:2067–75.
23. Prime RB. Differential scanning calorimetry of the epoxy cure reaction. Polym Eng Sci. 1973;13:365–71.
24. Riccardi CC, Dupuy J, Williams RJJ. A simple model to explain the complex kinetic behavior of epoxy/anhydride systems. J Polym Sci B: Polym Phys. 1999;37:2799–805.
25. Peyser P, Bascom WD. Kinetics of epoxy resin polymerization using differential scanning calorimetry. J Appl Polym Sci. 1977;21:2359–73.
26. González-Romero VM, Casillas N. Isothermal and temperature programmed kinetic studies of thermosets. Polym Eng Sci. 1989;29:295–301.
27. Khanna U, Chanda M. Kinetics of anhydride curing of isophthalic diglycidyl ester using differential scanning calorimetry. J Appl Polym Sci. 1993;49:319–29.
28. Hale A, Macosko CW, Bair HE. Glass transition temperature as a function of conversion in thermosetting polymers. Macromolecules. 1991;24:2610–21.
29. Mathew AP, Packirisamy S, Thomas S. Studies on the thermal stability of natural rubber/polystyrene interpenetrating polymer networks: thermogravimetric analysis. Polym Degrad Stab. 2001;72:423–39.
30. Gupta A, Singhal R, Nagpal AK. Reactive blends of epoxy resin (DGEBA) crosslinked by anionically polymerized polycaprolactam: process of epoxy cure and kinetics of decomposition. J Appl Polym Sci. 2004;92:687–97.